

Quantification of ^{18}F -florbetapir PET: comparison of two analysis methods

Chloe Hutton · Jerome Declerck · Mark A. Mintun ·
Michael J. Pontecorvo · Michael D. Devous Sr. ·
Abhinav D. Joshi · for the Alzheimer's Disease Neuroimaging Initiative

Received: 26 September 2014 / Accepted: 5 January 2015 / Published online: 5 February 2015
© Springer-Verlag Berlin Heidelberg 2015

Abstract

Purpose ^{18}F -Florbetapir positron emission tomography (PET) can be used to image amyloid burden in the human brain. A previously developed research method has been shown to have a high test-retest reliability and good correlation between standardized uptake value ratio (SUVR) and amyloid burden at autopsy. The goal of this study was to determine how well SUVRs computed using the research method could be reproduced using an automatic quantification method, developed for clinical use.

Methods Two methods for the quantitative analysis of ^{18}F -florbetapir PET were compared in a diverse clinical population of 604 subjects from the Alzheimer's Disease Neuroimaging Initiative (ADNI) and in a group of 74 younger healthy controls (YHC). Cortex to cerebellum SUVRs were calculated using the research method, which is based on SPM, yielding 'research SUVRs', and using syngo.PET Amyloid Plaque, yielding 'sPAP SUVRs'.

Results Mean cortical SUVRs calculated using the two methods for the 678 subjects were correlated ($r=0.99$). Linear regression of sPAP SUVRs on research SUVRs was used to convert the research method SUVR threshold for florbetapir positivity of 1.10 to a corresponding threshold of 1.12 for

sPAP. Using the corresponding thresholds, categorization of SUVR values were in agreement between research and sPAP SUVRs for 96.3 % of the ADNI images. SUVRs for all YHC were below the corresponding thresholds.

Conclusion Automatic florbetapir PET quantification using sPAP yielded cortex to cerebellum SUVRs which were correlated and in good agreement with the well-established research method. The research SUVR threshold for florbetapir positivity was reliably converted to a corresponding threshold for sPAP SUVRs.

Keywords Amyloid · Florbetapir · PET · Quantification · Alzheimer's disease

Introduction

A major histopathological hallmark of Alzheimer's disease (AD) is the deposition of β -amyloid neuritic plaques in the brain [1]. In vivo assessment of cortical β -amyloid burden can be performed using positron emission tomography (PET) imaging with amyloid imaging agents. Although the first human PET amyloid imaging was performed using ^{11}C -Pittsburgh compound B (PIB), [2], the short, 20-min half-life of ^{11}C limits its use to centres with an on-site cyclotron. In more recent years, ^{18}F -labelled PET tracers have been developed, and several studies have demonstrated their use in studies of neurodegenerative disorders and of aging [3–7].

With the translation of amyloid imaging from research to clinic, it is not surprising that much attention has been given to standardization of the technique in terms of imaging protocols, as well as guidelines for performing visual reads and image interpretation, to ensure appropriate use of amyloid imaging for routine clinical studies [8–10]. Consequently,

Data used in preparation of this article were obtained from the Alzheimer's Disease Neuroimaging Initiative (ADNI) database (adni.loni.usc.edu). As such, the investigators within the ADNI contributed to the design and implementation of ADNI and/or provided data but did not participate in analysis or writing of this report. A complete listing of ADNI investigators can be found at: http://adni.loni.usc.edu/wp-content/uploads/how_to_apply/ADNI_Acknowledgement_List.pdf

C. Hutton (✉) · J. Declerck
Siemens Molecular Imaging, Oxford, UK
e-mail: chloe.hutton@siemens.com

M. A. Mintun · M. J. Pontecorvo · M. D. Devous Sr. · A. D. Joshi
Avid Radiopharmaceuticals a wholly owned subsidiary of Eli Lilly and Company, Philadelphia, PA, USA

there has also been an increased interest in developing simple, accurate and reproducible methods for quantification of amyloid PET data which can potentially provide additional diagnostic information when used as an adjunct to the visual read.

The first study to propose a simple quantification method for amyloid PET data involved the calculation of standardized uptake value ratios (SUVRs) between cortical target regions and a reference region, where the regions were defined on MR images coregistered to the PET image [11]. These early studies relied on manual delineation of the regions of interest (ROIs) [e.g. 11, 12]. More recent studies [e.g. 4, 13, 14] employed an approach to quantification of β -amyloid burden that involves registration of the PET image to a standard template space so that SUVs can be computed automatically from target and reference regions, which have been predefined and delineated in the template space. A single composite SUVR is then typically computed from the average of the individual SUVs relative to a reference region of choice. Automatic quantification using predefined anatomical regions should improve reproducibility, but the precise definition and location of proposed reference and target regions has varied between studies.

For florbetapir quantification, the previously developed and well-established research method has been shown to yield SUVs with high test–retest reliability and was used to introduce an SUVR threshold for florbetapir positivity to β -amyloid [15]. In a following study, this method was also used to compare SUVs with neuropathology at autopsy and showed that all but 1 of the 59 cases with moderate or frequent plaques at autopsy had a composite SUVR greater than the proposed florbetapir positivity threshold [14].

The goal of the current study was therefore to determine how well SUVs computed with the established research method could be reproduced by syngo.PET Amyloid Plaque (sPAP), an automatic quantification method developed for clinical use [16]. The latter method uses a different registration approach and independently defined reference and target regions to the research method. To compare the two approaches, cortex to cerebellum SUVs were calculated using sPAP and the research method in a diverse clinical population of 604 subjects from the Alzheimer's Disease Neuroimaging Initiative (ADNI) database (<http://adni.loni.ucla.edu>). The two methods were also used to compute and compare SUVs for florbetapir PET data from a group of 74 younger healthy controls (YHC).

Materials and methods

ADNI data

Data used in the preparation of this article were obtained from the ADNI database (adni.loni.usc.edu). The ADNI was

launched in 2003 by the National Institute on Aging (NIA), the National Institute of Biomedical Imaging and Bioengineering (NIBIB), the US Food and Drug Administration (FDA), private pharmaceutical companies and non-profit organizations, as a \$60 million, 5-year public-private partnership. The primary goal of ADNI has been to test whether serial magnetic resonance imaging (MRI), PET, other biological markers, and clinical and neuropsychological assessment can be combined to measure the progression of mild cognitive impairment (MCI) and early AD. Determination of sensitive and specific markers of very early AD progression is intended to aid researchers and clinicians to develop new treatments and monitor their effectiveness, as well as lessen the time and cost of clinical trials.

The Principal Investigator of this initiative is Michael W. Weiner, M.D., VA Medical Center and University of California, San Francisco. ADNI is the result of efforts of many coinvestigators from a broad range of academic institutions and private corporations, and subjects have been recruited from over 50 sites across the USA and Canada. The initial goal of ADNI was to recruit 800 subjects but ADNI has been followed by ADNI-GO and ADNI-2. To date these three protocols have recruited over 1,500 adults, aged 55–90, to participate in the research, consisting of cognitively normal older individuals, people with early or late MCI and people with early AD. The follow-up duration of each group is specified in the protocols for ADNI-1, ADNI-2 and ADNI-GO. Subjects originally recruited for ADNI-1 and ADNI-GO had the option to be followed in ADNI-2. For up-to-date information, see www.adni-info.org.

Participants

Florbetapir PET images from 604 participants were downloaded from ADNI (<http://adni.loni.usc.edu>), representing all available florbetapir PET images as of August 2012. Subjects were clinically diagnosed as normals (NL, $n=200$), early mild cognitively impaired (EMCI, $n=215$), mild cognitively impaired (MCI, $n=163$) and AD ($n=26$), according to the diagnosis given at the closest time to the florbetapir PET scan date. Images were downloaded in their most fully post-reconstruction processed format. This corresponds to a series description in the ADNI Advanced Search of “AV45 Coreg, Avg, Std Img and Vox Siz, Uniform Resolution”. Full details of the processing steps can be found online (<http://adni.loni.usc.edu/methods/pet-analysis/pre-processing/>), but in summary they included coregistration and averaging of the individual PET frames and orientation to the AC-PC line. Image acquisition is also described in detail online (http://adni.loni.ucla.edu/wp-content/uploads/2010/05/ADNI2_PET_Tech_Manual_0142011.pdf), but briefly, participants were intravenously injected with 370 MBq (\pm

10 %) of florbetapir and imaged for 20 min starting 50 min after radiotracer injection.

Also used were the florbetapir PET images acquired from 74 young cognitively normal, healthy individuals (YHC, aged 18–50 years). According to age these subjects should have no β -amyloid neuritic plaques, classified based on the Consortium to Establish a Registry on Alzheimer's Disease (CERAD).

Calculation of SUVR using semiautomated research method

The research method used the nonlinear registration algorithm from SPM2 [17] to register florbetapir PET images to a florbetapir PET template in MNI space [18]. The previously developed florbetapir template was an average of 10-min florbetapir images acquired at 50 min after injection from 15 healthy normal and 11 clinically diagnosed AD subjects obtained in a previous study [19]. An initial nonlinear registration to the template was applied to all data and was referred to as fit 1. The registration results were visually checked for alignment to the template brain. Cases with unacceptable results from fit 1 were registered using a weighting factor in the form of a template brain mask, so that only voxels within the brain were used to optimize the registration; this method was referred to as fit 2. Cases with unacceptable results from fit 2 were registered using fit 3, which includes skull-stripping the patient image. Skull-stripping was performed using the brain extraction tool kit (BET) in MRIcro (version 1.40 Build 1), with a fractional intensity ranging from 0.5 to 0.65. The skull-stripped image was then spatially normalized to the MNI space and the transformation was applied to the original patient PET image. Cases with acceptable registration results, based on visual examination, were used for SUVR calculation.

Research SUVRs were calculated from the mean uptake value in six cortical ROIs (medial orbital frontal, parietal, temporal, precuneus, posterior cingulate and anterior cingulate) with respect to the mean uptake in the entire cerebellum as a reference region. The whole cerebellum was selected as the reference region because it has been shown to contain negligible levels of fibrillar amyloid and low levels of PIB binding in postmortem binding studies of subjects with different dementia diagnoses (e.g. see [11]). In other studies, [e.g. 4, 12], cerebellar cortex was used as the reference region, but as it contains a very fine organization of grey and white matter, accurate registration and delineation may be more challenging than for the whole cerebellum.

A composite SUVR was calculated from the average of the six individual SUVRs. The six target ROIs were defined in a previous study [13], using a combination of the Automated Anatomical Labelling (AAL) atlas [20] and manual delineation within grey matter regions (defined using segmented MRI) where PET uptake was increased in AD subjects

compared with control subjects. The previously defined cerebellum region in MNI brain space was used as a reference region [13].

Calculation of SUVR using sPAP

sPAP [16] uses affine registration to register florbetapir PET images to a synthetic PET template, which was created to resemble an average set of florbetapir PET images. The synthetic PET template was created from 19 T1-weighted MR images from older healthy subjects. Bias-field correction and tissue classification were performed on each MR volume using a Siemens in-house segmentation tool based on a variational expectation maximization algorithm [21]. This step resulted in segmented images of grey matter, white matter and CSF. The segmented images were also transformed to the reference space and averaged together to create grey matter, white matter and CSF probability maps. The tissue probability maps were combined with different weights and smoothed to create a synthetic PET template image which resembled an average (between healthy and diseased) amyloid PET image. The reference brain was then manually registered to MNI space and the resulting affine transformation was applied to the synthetic PET template image.

Registration results were visually examined by comparing alignment of the patient's PET brain to the template brain and alignment of the patient cerebellum to the template cerebellum outline. For cases requiring an improvement to the automatic registration results, manual registration adjustments were applied using a 12 parameter affine transformation tool, which allows for translation, scaling, rotation and shearing.

As with the research method, sPAP SUVRs were calculated from the mean uptake values in medial orbital frontal, parietal, temporal, precuneus, anterior and posterior cingulate with whole cerebellum as a reference region. A composite SUVR was also computed from the average of the six regional SUVR values. Although sPAP used the same nominal regions as the research method, the precise region delineation was made independently. In the sPAP case, the corresponding AAL atlas regions were used as a starting point. The grey matter probability image from the synthetic PET template was used to mask the AAL ROIs and manual editing was applied so they were visually similar to those presented in [13]. Note that sPAP regions were defined prior to this comparative study.

Results

For both the research and sPAP methods, all 604 ADNI subjects were successfully registered to MNI space according to visual inspection. Using the research method, 15/604 cases (2.5 %) required additional preprocessing (10 required fit 2

and 5 required fit 3) for successful registration. Using sPAP, 14/604 cases (2.3 %) required manual registration adjustments to the initial automatic registration. Using both methods, all 74 YHC subjects were also successfully registered to MNI space according to visual inspection. Using sPAP, 6/74 YHC subjects required manual adjustments to improve the registration to the template and using the research method, 13/74 cases required additional processing (12 required fit 2 and 1 required fit 3).

Mean cortical SUVRs from all 678 subjects using the two methods were correlated ($r=0.99$) over the range from 0.77 to 2.25 (Fig. 1). The linear regression of sPAP SUVRs on research SUVRs was $y=0.980*x+0.039$. The regression equation was used to convert the research proposed SUVR threshold for florbetapir positivity (SUVR>1.10, [15]) to a corresponding threshold for sPAP (SUVR>1.12). Using the corresponding thresholds, categorization of SUVR values was in agreement between research and sPAP SUVR for 96.8 % of the images, with 272/678 (40.1 %) in the positive range and 384/678 (56.6 %) in the negative range. In 7 images (1.0 %) only the research method SUVR was classified as positive and in 15 images (2.2 %) only sPAP SUVR was classified as positive. This categorization corresponds to a Cohen's kappa coefficient, $\kappa=0.93$. For the 14 ADNI cases which required manual registration adjustments with sPAP, the adjustments were performed by two independent operators and the categorization of SUVR values was in agreement between operators for all but 1 subject (i.e. 93 % agreement). Note that considering the 74 YHC subjects alone, SUVRs ranged from 0.87 to 1.08 (yellow circles, Fig. 1) and were all categorized as negative using both methods.

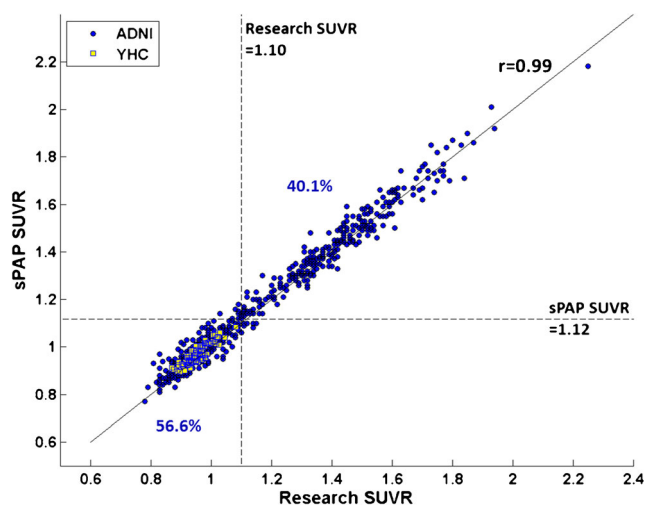


Fig. 1 sPAP SUVR values plotted against research SUVR values for 604 ADNI subjects (blue circles) and 74 YHC (yellow circles). The correlation between sPAP and research SUVRs for all 678 subjects is $r=0.99$. The percentages of cases for which the categorization of sPAP and research SUVRs were in agreement for the positive and negative ranges of SUVRs are shown in blue

The mean and standard deviations of the composite and individual regions for ADNI subjects categorized as positive and negative using the thresholds are shown in Table 1. Two examples of florbetapir PET images registered in MNI space using sPAP with target and reference regions displayed as contours are shown in Fig. 2. For these examples, research and sPAP methods yielded the same composite SUVRs. The image on the left has a composite SUVR=0.89 and the image on the right has a composite SUVR=1.77.

The agreement between research and sPAP composite SUVRs is also illustrated using a Bland-Altman plot (Fig. 3), which plots SUVR difference against SUVR average for the two methods. The mean (SD) difference between research and sPAP SUVRs was 0.02 (0.04), and 95 % limits of agreement were -0.06 to 0.09 . The mean (SD) difference for the 51.3 % of images in the negative range was 0.02 (0.03) and for the 45 % of images in the positive range was 0.01 (0.04). To determine whether there was a significant linear relationship between the performance of the two methods and SUVR value, the SUVR difference values were regressed on the SUVR mean values. Using a two-tailed t test, the slope of the resulting regression line was found to be not significantly different from zero ($p>0.05$).

The seven subjects (1.0 %) whose images were classified as amyloid positive using the research method and amyloid negative using sPAP had been given diagnoses at the time of the florbetapir scan of MCI ($n=1$), EMCI ($n=4$) and NL ($n=2$). The 15 subjects whose images were classified as amyloid positive using sPAP and amyloid negative using the research method had diagnoses of MCI ($n=5$), EMCI ($n=8$) and NL ($n=2$).

Discussion

In this study we have shown that the sPAP software provides cortex to cerebellum composite SUVRs which are correlated ($r=0.99$) and are in good agreement ($\kappa=0.93$) with the research method. Importantly the two methods use different approaches to registration, including different registration templates and similar but not identical target and reference ROIs for SUVR computation. The accuracy of the quantification depends on how accurately the ROIs are positioned and therefore on the accuracy of the registration method. A number of studies have used nonlinear registration of PET data to a PET template [4, 13, 15, 19, 22]. In contrast, sPAP uses affine registration of PET images to a synthetic PET template.

For this study, it is important to note that the ADNI data were acquired and reconstructed similarly and according to strict protocols. The ADNI protocols describe specific acquisition and reconstruction parameters for a range of scanner manufacturers and models, to ensure consistency across different scanners and data collection. If data were acquired and

Table 1 Mean (standard deviation) of positive and negative SUVRs for composite and individual regions for ADNI subjects

Region	Research SUVR		sPAP SUVR		Difference positive mean (SD)	Difference negative mean (SD)	Correlation (<i>r</i>)
	Positive mean (SD)	Negative mean (SD)	Positive mean (SD)	Negative mean (SD)			
Composite	1.42 (0.19)	0.96 (0.19)	1.42 (0.19)	0.97 (0.19)	0.01 (0.04)	0.02 (0.04)	0.99
Frontal	1.25 (0.18)	0.87 (0.18)	1.29 (0.21)	0.87 (0.21)	0.05 (0.07)	0.00 (0.05)	0.97
Temporal	1.44 (0.20)	1.03 (0.20)	1.51 (0.19)	1.13 (0.19)	0.08 (0.06)	0.10 (0.06)	0.97
Anterior cingulate	1.49 (0.24)	0.97 (0.24)	1.40 (0.22)	0.93 (0.22)	-0.08 (0.07)	-0.04 (0.07)	0.97
Posterior cingulate	1.42 (0.22)	0.95 (0.22)	1.49 (0.22)	1.00 (0.22)	0.07 (0.11)	0.06 (0.09)	0.94
Parietal	1.30 (0.20)	0.90 (0.20)	1.31 (0.19)	0.94 (0.19)	0.02 (0.13)	0.04 (0.11)	0.89
Precuneus	1.59 (0.24)	1.04 (0.24)	1.54 (0.25)	0.98 (0.25)	-0.04 (0.09)	0.06 (0.08)	0.97

The data from each subject were assigned to the positive or negative group on the basis of the composite SUVR > 1.10 for the research method and SUVR > 1.12 for sPAP. The correlation (*r*) was calculated for SUVR values over all subjects for each region

reconstructed using other (non-ADNI recommended) protocols, there may be an effect on image appearance and pixel values leading to different registration and SUVR results. In a previous study [23], reasonable robustness to reconstruction parameters and method was demonstrated using sPAP to compare florbetapir images reconstructed using point spread

function (PSF), time of flight (TOF) and ordered subset expectation maximization (OSEM). Although not explicitly tested, the results of the previous and current studies suggest that the effect of reconstruction on the agreement between sPAP and research SUVRs should not be significant. The post-reconstruction processed format (ADNI, stage 4) of the PET

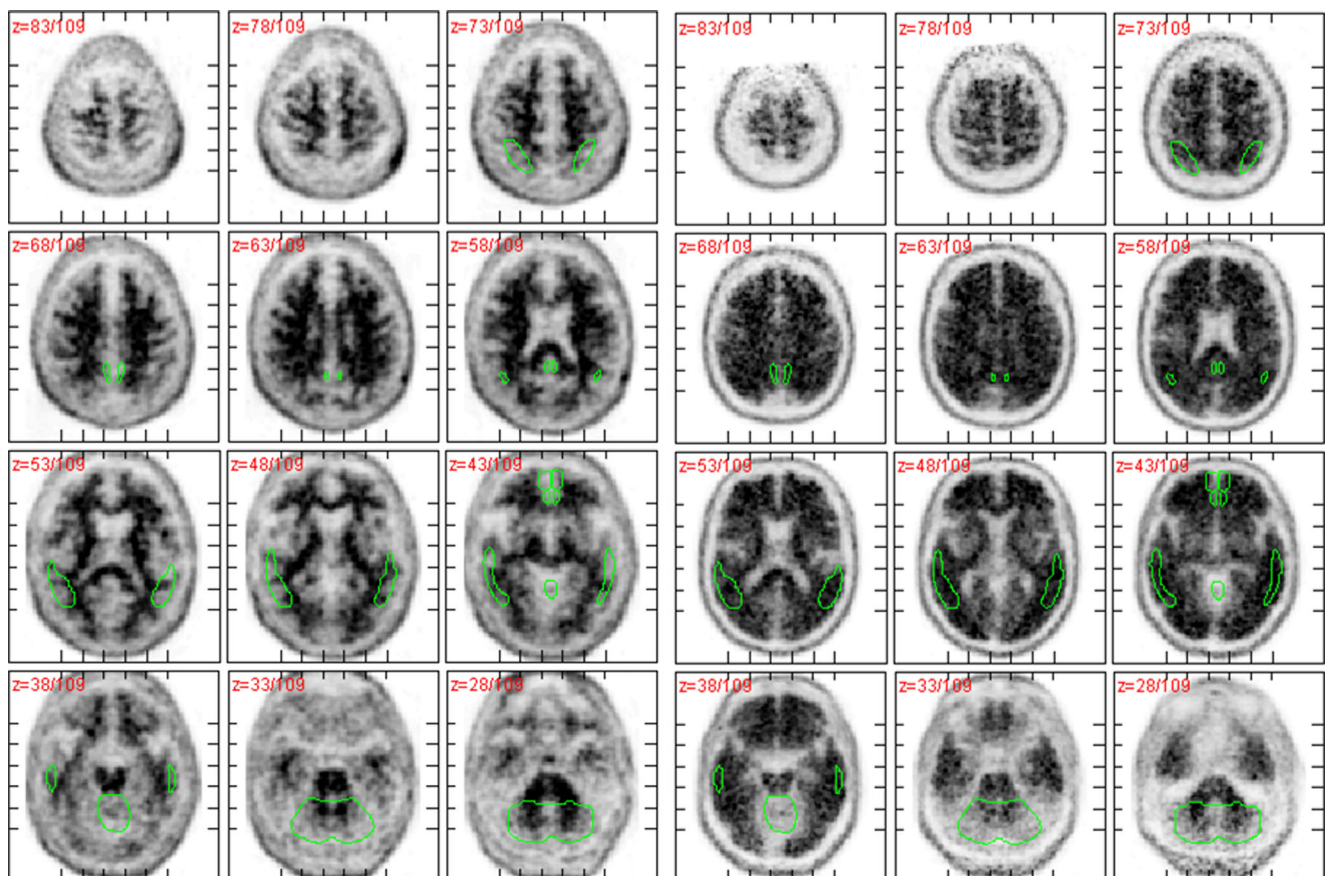


Fig. 2 Two examples of florbetapir PET images registered to MNI space using sPAP, with reference and target regions outlined in green. For these examples, research and sPAP methods yielded the same composite

SUVRs. The image on the left has a composite SUVR=0.89 (below the thresholds) and the image on the right has a composite SUVR=1.77 (above the thresholds)

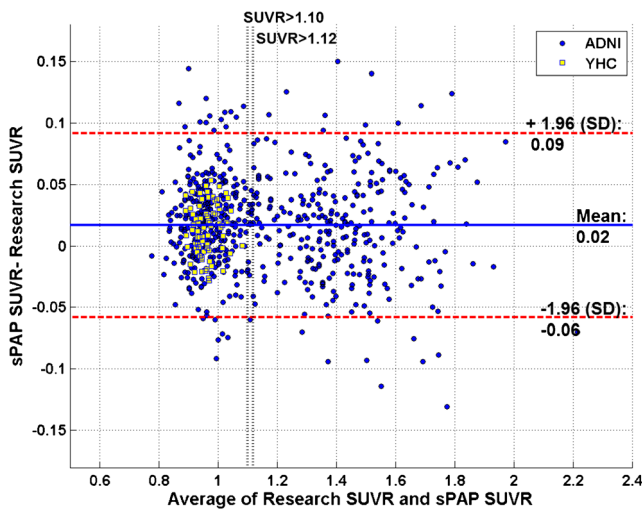


Fig. 3 Bland-Altman plot showing the difference between sPAP and research SUVR values plotted against their average. The *solid horizontal line* shows the mean SUVR difference of 0.02 and the *dotted lines* show the 95 % confidence limits

images analysed in this study is not required for sPAP to work successfully; the initial study evaluating sPAP in a group of 210 non-preprocessed florbetapir PET images [16] resulted in SUVRs comparable to those published in [13]. However, the quality of clinical PET data from routine clinical practice is likely to be more variable, which may have an impact on registration performance. It is therefore important that processing software like sPAP allow for easy review of registration results and manual adjustments to the registration if required.

A particular challenge for the registration of amyloid PET images is that the uptake pattern and contrast are very different between cases with lower and higher amyloid burden, which may lead to different registration performance between positive and negative cases. To account for this effect, an adaptive template registration method was proposed in [24] that generates the optimal template for the uptake level of the input PET image. In the current study, no significant difference was found in the agreement between research and sPAP SUVRs for positive and negative cases. This suggests that the two methods performed similarly for positive and negative cases.

Alternative approaches to quantification have been used when the patient data include an MRI, for example, an individualized definition of grey matter can be created from MRI segmentation [4] or by parcellating the MRI into different brain regions [6, 25]. Notably, a study comparing PIB PET SUVRs obtained using PET-only with MR-based registration concluded that the methods provided comparable quantitative measures, which are adequate for clinical purposes [22]. An advantage of the methods compared in this study is that they rely only on the patient PET image for processing and do not require an MRI for registration or delineation of regions. This is important when considering that for routine clinical studies the quantification method should be simple and practical to

use, and obtaining an appropriate patient MRI may be unfeasible.

The linear regression of ADNI sPAP composite SUVRs on research SUVRs was used to convert the proposed research SUVR threshold for florbetapir positivity to a corresponding threshold for sPAP. This scaling procedure allowed for the categorization of SUVRs obtained using a new quantification method without performing an additional study to determine the positivity threshold for the new method. For the YHC data, all SUVRs were less than the corresponding research and sPAP thresholds for positivity. A similar threshold scaling procedure was used in a comparison study between two different β -amyloid radiotracers and quantification methods, where the study cohort were scanned with both tracers [6]. A further study [26] compared data from two cohorts, one scanned with florbetapir and PIB and the other with flutemetamol and PIB. In both studies the authors concluded that cut-offs for establishing positive and negative β -amyloid status could be accurately transformed between radiotracers and processing methods. In general, the quantification of amyloid data can yield variable results across different studies as a consequence of data acquisition on different scanners as well as using different radiotracers and analysis methods. Therefore the standardization of quantification methods is important to facilitate comparisons across different amyloid PET studies and for practical clinical application of thresholds for amyloid positivity. A more general proposal to standardize quantitative amyloid imaging is the “centiloid project” [e.g. see 27], which defines a procedure where PIB PET data acquired in a group of young controls and typical AD patients are analysed using a standard method and the results are used to define the anchor points of the centiloid scale. Results obtained using any method other than the “standard” method can then be converted to the centiloid scale using a linear regression process much like that described here.

It should be noted that even with standardization of amyloid PET quantification the quantitative value should serve as an adjunct to visual reading of the PET images, and amyloid status determined from the PET image cannot be used to establish a diagnosis of AD or other cognitive disorder. We believe that the results of this study contribute to the issue of standardization of amyloid PET image processing and analysis by demonstrating the reproducibility of the florbetapir PET cortex to cerebellum SUVR quantification method as initially established by Avid Radiopharmaceuticals. Similar studies can be performed to establish the reproducibility of amyloid quantification methods using alternative approaches and different radiotracers.

Conclusion

We have shown that the two methods yield quantitative results that are highly correlated (96.3 % for the ADNI data) and in

good agreement. Additionally, the sPAP method (like the research method) did not yield any positive results in the group of cognitively normal young subjects.

Acknowledgments Data collection and sharing for this project was funded by the Alzheimer's Disease Neuroimaging Initiative (ADNI) (National Institutes of Health Grant U01 AG024904) and DOD ADNI (Department of Defense award number W81XWH-12-2-0012). ADNI is funded by the National Institute on Aging, the National Institute of Biomedical Imaging and Bioengineering, and through generous contributions from the following: Alzheimer's Association; Alzheimer's Drug Discovery Foundation; Araclon Biotech; BioClinica, Inc.; Biogen Idec Inc.; Bristol-Myers Squibb Company; Eisai Inc.; Elan Pharmaceuticals, Inc.; Eli Lilly and Company; EuroImmun; F. Hoffmann-La Roche Ltd and its affiliated company Genentech, Inc.; Fujirebio; GE Healthcare; IXICO Ltd.; Janssen Alzheimer Immunotherapy Research & Development, LLC.; Johnson & Johnson Pharmaceutical Research & Development LLC.; Medpace, Inc.; Merck & Co., Inc.; Meso Scale Diagnostics, LLC.; NeuroRx Research; Neurotrack Technologies; Novartis Pharmaceuticals Corporation; Pfizer Inc.; Piramal Imaging; Servier; Synarc Inc.; and Takeda Pharmaceutical Company. The Canadian Institutes of Health Research is providing funds to support ADNI clinical sites in Canada. Private sector contributions are facilitated by the Foundation for the National Institutes of Health (www.fnih.org). The grantee organization is the Northern California Institute for Research and Education, and the study is coordinated by the Alzheimer's Disease Cooperative Study at the University of California, San Diego. ADNI data are disseminated by the Laboratory for Neuro Imaging at the University of Southern California.

Compliance with ethical standards

Conflicts of interest Chloe Hutton and Jerome Declerck are employees of Siemens Healthcare Molecular Imaging. Mark A. Mintun, Michael J. Pontecorvo, Michael D. Devous, Sr., and Abhinav D. Joshi are employees of Avid Radiopharmaceuticals Inc., a wholly owned subsidiary of Eli Lilly and company.

Human participants Data used in this study were obtained from the Alzheimer's Disease Neuroimaging Initiative (ADNI) database with agreement under the terms of the ADNI Data Use Agreement. Submission of data to the ADNI database was approved by the Institutional Review Boards of all of the participating institutions. Informed written consent was obtained from all participants at each site.

References

- Hardy J, Selkoe DJ. The amyloid hypothesis of Alzheimer's disease: progress and problems on the road to therapeutics. *Science* 2002;297(5580):353–6.
- Klunk WE, Engler H, Nordberg A, Wang Y, Blomqvist G, Holt DP, et al. Imaging brain amyloid in Alzheimer's disease with Pittsburgh Compound-B. *Ann Neurol* 2004;55(3):306–19.
- Vandenberghe R, Van Laere K, Ivanoiu A, Salmon E, Baslin C, Triau E, et al. 18F-flutemetamol amyloid imaging in Alzheimer disease and mild cognitive impairment: a phase 2 trial. *Ann Neurol* 2010;68(3):319–29.
- Barthel H, Gertz H-J, Dresel S, Peters O, Bartenstein P, Buerger K, et al. Cerebral amyloid- β PET with florbetaben (18F) in patients with Alzheimer's disease and healthy controls: a multicentre phase 2 diagnostic study. *Lancet Neurol* 2011;10(5):424–35.
- Clark CM, Schneider JA, Bedell BJ, Beach TG, Bilker WB, Mintun MA, et al. Use of florbetapir-PET for imaging beta-amyloid pathology. *JAMA* 2011;305(3):275–83.
- Landau SM, Breault C, Joshi AD, Pontecorvo M, Mathis CA, Jagust WJ, et al. Amyloid- β imaging with Pittsburgh compound B and florbetapir: comparing radiotracers and quantification methods. *J Nucl Med* 2013;54(1):70–7.
- Rowe CC, Pejoska S, Mulligan RS, Jones G, Chan JG, Svensson S, et al. Head-to-head comparison of 11C-PiB and 18F-AZD4694 (NAV4694) for β -amyloid imaging in aging and dementia. *J Nucl Med* 2013;54(6):880–6.
- Johnson KA, Minoshima S, Bohnen NI, Donohoe KJ, Foster NL, Herscovitch P, et al. Appropriate use criteria for amyloid PET: a report of the Amyloid Imaging Task Force, the Society of Nuclear Medicine and Molecular Imaging, and the Alzheimer's Association. *J Nucl Med* 2013;54(3):476–90.
- Booij J, Arbizu J, Darcourt J, Hesse S, Nobili F, Payoux P, et al. Appropriate use criteria for amyloid PET imaging cannot replace guidelines: on behalf of the European Association of Nuclear Medicine. *Eur J Nucl Med Mol Imaging* 2013;40(7):1122–5.
- Rowe CC, Villemagne VL. Brain amyloid imaging. *J Nucl Med* 2011;52(11):1733–40.
- Lopresti BJ, Klunk WE, Mathis CA, Hoge JA, Ziolkowski SK, Lu X, et al. Simplified quantification of Pittsburgh compound B amyloid imaging PET studies: a comparative analysis. *J Nucl Med* 2005;46(12):1959–72.
- Rowe CC, Ackerman U, Browne W, Mulligan R, Pike KL, O'Keefe G, et al. Imaging of amyloid beta in Alzheimer's disease with 18F-BAY94-9172, a novel PET tracer: proof of mechanism. *Lancet Neurol* 2008;7(2):129–35.
- Fleisher AS, Chen K, Liu X, Roontiva A, Thiyyagura P, Ayutyanont N, et al. Using positron emission tomography and florbetapir F18 to image cortical amyloid in patients with mild cognitive impairment or dementia due to Alzheimer disease. *Arch Neurol* 2011;68(11):1404–11.
- Clark CM, Pontecorvo MJ, Beach TG, Bedell BJ, Coleman RE, Doraiswamy PM, et al. Cerebral PET with florbetapir compared with neuropathology at autopsy for detection of neuritic amyloid- β plaques: a prospective cohort study. *Lancet Neurol* 2012;11(8):669–78.
- Joshi AD, Pontecorvo MJ, Clark CM, Carpenter AP, Jennings DL, Sadowsky CH, et al. Performance characteristics of amyloid PET with florbetapir F 18 in patients with Alzheimer's disease and cognitively normal subjects. *J Nucl Med* 2012;53(3):378–84.
- Peyrat J-M, Joshi A, Mintun M, Declerck J. An automatic method for the quantification of uptake with florbetapir imaging. Miami: Society of Nuclear Medicine; 2012.
- Friston KJ, Ashburner JT, Kiebel SJ, Nichols TE, Penny WD, editors. *Statistical parametric mapping: the analysis of functional brain images*. London: Academic; 2007.
- Evans A, Collins DL, Mills SR, Brown ED, Kelly RL, Peters TM. 3D statistical neuroanatomical models from 305 MRI volumes. *IEEE Nucl Sci Symp Med Imag Conf* 1993;1813–1817.
- Wong DF, Rosenberg PB, Zhou Y, Kumar A, Raymont V, Ravert HT, et al. In vivo imaging of amyloid deposition in Alzheimer disease using the radioligand 18F-AV-45 (florbetapir [corrected] F 18). *J Nucl Med* 2010;51(6):913–20.
- Tzourio-Mazoyer N, Landeau B, Papathanassiou D, Crivello F, Etard O, Delcroix N, et al. Automated anatomical labeling of activations in SPM using a macroscopic anatomical parcellation of the MNI MRI single-subject brain. *Neuroimage* 2002;15(1):273–89.
- Roche A, Ribes D, Bach-Cuadra M, Kruger G. On the convergence of EM-like algorithms for image segmentation using Markov random fields. *Med Image Anal* 2011;15(6):830–9.

22. Edison P, Carter SF, Rinne JO, Gelosa G, Herholz K, Nordberg A, et al. Comparison of MRI based and PET template based approaches in the quantitative analysis of amyloid imaging with PIB-PET. *Neuroimage* 2013;70:423–33.
23. Peyrat J-M, Joshi A, Mintun M, Declercq J. Influence of reconstruction methods and parameters in quantification of uptake with florbetapir imaging. Milan: EANM; 2012.
24. Lundqvist R, Lilja J, Thomas B, Lötjönen J, Villemagne VL, Rowe CC, et al. Implementation and validation of an adaptive template registration method for 18F-flutemetamol imaging data. *J Nucl Med* 2013;54(8):1472–8.
25. Thomas BA, Erlandsson K, Modat M, Thurfjell L, Vandenberghe R, Ourselin S, et al. The importance of appropriate partial volume correction for PET quantification in Alzheimer's disease. *Eur J Nucl Med Mol Imaging* 2011;38(6):1104–19.
26. Landau SM, Thomas BA, Thurfjell L, Schmidt M, Margolin R, Mintun M, et al. Amyloid PET imaging in Alzheimer's disease: a comparison of three radiotracers. *Eur J Nucl Med Mol Imaging* 2014;41:1398–407.
27. Klunk WE, Koeppe RA, Price JC, Benzinger TL, Devous MD, Jagut WJ, et al. The centiloid project: standardizing quantitative amyloid plaque estimation by PET. *Alzheimers Dementia*. doi: [10.1016/j.jalz.2014.07.003](https://doi.org/10.1016/j.jalz.2014.07.003).